Dexamethasone Attenuates the Enhanced Rewarding Effects of Cocaine Following Experimental Traumatic Brain Injury

Steven F. Merkel[1,2]**, Allison M. Andrews**[1,2]**, Evan M. Lutton**[1]**, Roshanak Razmpour**[1]**, Lee Anne Cannella**[1,2]**, and Servio H. Ramirez**[1,2,3]

Abstract

Clinical studies have identified traumatic brain injury (TBI) as a risk factor for the development of cocaine dependence. This claim is supported by our recent preclinical studies showing enhancement of the rewarding effects of cocaine in mice sustaining moderate controlled cortical impact (CCI) injury during adolescence. Here we test the efficacy of dexamethasone, an anti-inflammatory corticosteroid, to attenuate augmentation of the behavioral response to cocaine observed in CCI-TBI animals using the conditioned place preference (CPP) assay. These studies were performed in order to determine whether proinflammatory activity in the nucleus accumbens (NAc), a key brain nucleus in the reward pathway, mediates enhanced cocaine-induced CPP in adolescent animals sustaining moderate CCI-TBI. Our data reveal robust glial activation in the NAc following CCI-TBI and a significant increase in the cocaine-induced CPP of untreated CCI-TBI mice. Furthermore, our results show that dexamethasone treatment following CCI-TBI can attenuate the cocaine place preference of injured animals without producing aversion in the CPP assay. Our studies also found that dexamethasone treatment significantly reduced the expression of select immune response genes including Monocyte chemoattractant protein-1 (MCP-1/CCL2) and intercellular adhesion molecule-1 (*ICAM-1*), returning their expression to control levels, which prompted an investigation of peripheral blood monocytes in dexamethasone-treated animals. Experimental findings showed that no craniectomy/dexamethasone mice had a significant increase, while CCI-TBI/dexamethasone animals had a significant decrease in the percentage of circulating nonclassical patrolling monocytes. These results suggest that a portion of these monocytes may migrate to the brain in response to CCI-TBI, potentially sparing the development of chronic neuroinflammation in regions associated with the reward circuitry such as the NAc. Overall, our findings indicate that anti-inflammatory agents, such as dexamethasone, may be effective in normalizing the rewarding effects of cocaine following CCI-TBI.

Keywords

traumatic brain injury, nucleus accumbens, conditioned place preference, cocaine, dexamethasone

Introduction

Substance abuse is the third most common neuropsychiatric complication among patients with a history of traumatic brain injury (TBI).[1] Recent reports have identified adolescent TBI patients as particularly vulnerable to problematic alcohol and illicit drug use.[2] Specifically, in the context of cocaine addiction, clinical studies have shown that 84% of cocaine-dependent research volunteers sustained their first TBI (mean age: 16) prior to initiating cocaine use (mean age: 23).[3] Furthermore, using preclinical animal models, our recent report, Merkel et al. show that adolescent mice with a history of moderate controlled cortical impact (CCI) injury exhibit greater susceptibility to the rewarding effects of cocaine in a conditioned place preference (CPP) assay compared to controls.[4]

[1] Department of Pathology and Laboratory Medicine, The Lewis Katz School of Medicine at Temple University, Philadelphia, PA, USA
[2] Center for Substance Abuse Research, The Lewis Katz School of Medicine at Temple University, Philadelphia, PA, USA
[3] Shriners Hospitals Pediatric Research Center, The Lewis Katz School of Medicine at Temple University, Philadelphia, PA, USA

Corresponding Author:
Servio H. Ramirez, Department of Pathology and Laboratory Medicine, The Lewis Katz School of Medicine at Temple University, 3500 N. Broad St. MERB 844, Philadelphia, PA 19140, USA.
Email: servio@temple.edu

Cocaine addiction is believed to be partly the result of dysfunction in the mesolimbic pathway, consisting of the nucleus accumbens (NAc) and ventral tegmental area.[5,6] These brain nuclei mediate the rewarding and euphoric effects of cocaine, although the exact mechanism regulating cocaine dependence remains unknown. Notably, current studies in substance abuse research suggest that the expression of innate immune factors in the NAc may mediate drug and alcohol abuse behavior.[7–12] Our recent data demonstrated overexpression of numerous immune response genes in the NAc following CCI-TBI.[4] Therefore, in the current study, we hypothesize that neuroinflammation in the NAc mediates the augmentation of cocaine place preference following moderate, adolescent CCI-TBI.

To test this hypothesis, we selected dexamethasone as a steroidal, anti-inflammatory therapy to examine whether diminishing the immune response following CCI-TBI could attenuate enhancement of the rewarding effects of cocaine exhibited by CCI-TBI mice during a 3-phase CPP assay. Using multiphoton microscopy, our data reveal acute and chronic glial activation in the NAc following moderate CCI-TBI. Furthermore, administering dexamethasone following CCI-TBI significantly reduced the enhanced response to cocaine displayed by CCI-TBI/untreated animals and returned cocaine place preference to the level of no craniectomy controls. Dexamethasone treatment also significantly reduced the expression of select immune response genes in the NAc including *CCL2* and *ICAM-1* when compared to CCI-TBI/untreated animals, prompting investigation of peripheral blood monocytes.

Monocytes are known to respond and infiltrate the brain during neuroinflammation, excitotoxicity,[13] ischemia,[14] and TBI.[15,16] Three specific monocyte populations have been identified in both humans and mice based on cell surface markers and specific subset functions.[17] Murine monocytes are identified on their differential expression of Ly6C (lo, med, hi).[17,18] Ly6C^{hi} monocytes or classical monocytes are known for their response to inflammatory signals and phagocytic functions,[17] and their role in chronic inflammation.[19] Ly6C^{med} monocytes or intermediate monocytes, such as Ly6C^{hi} classical monocytes, respond to proinflammatory cues and are recruited to inflammatory lesions where they differentiate into macrophages.[20] The third subtype, Ly6C^{lo} or nonclassical monocytes patrol the vasculature under homeostatic and inflammatory conditions and can initiate the repair of the tissue.[17,19,21] Additionally, nonclassical monocytes have been shown to remove damaged cells and debris from the vasculature[22] and are thought to replenish the tissue-resident macrophage and dendritic cell populations.[23,24] Recent studies have examined changes in some monocytes subtypes following TBI,[25,26] however, the specific importance of nonclassical/patrolling monocytes has yet to be explored in context of TBI. In addition, strategies to alter monocyte phenotypes in order to shift the immune response away from chronic inflammation to speed resolution in the tissue have never been explored.

In this report, we show that dexamethasone treatment shifted the profile of monocytes, increasing the pool of the Ly6C^{med} (intermediate) and Ly6C^{lo} (nonclassical or patrolling) monocytes and significantly reduced the population of Ly6C^{hi} (classical, inflammatory) monocytes present in the blood. Interestingly, although CCI-TBI or dexamethasone alone did not change the total number of monocytes in the blood, the combination of CCI-TBI and dexamethasone exhibited a significant reduction in the percentage of total monocytes, specifically, nonclassical patrolling monocytes in the blood. Together, these results suggest that dexamethasone treatment following moderate CCI-TBI may attenuate increased vulnerability to the rewarding effects of cocaine, possibly by shifting the profile of immune cells responding to damage in the brain, thus sparing chronic neuroinflammation in brain nuclei distal to the site of injury, such as the NAc.

Materials and Methods

Animals

For histology, real-time polymerase chain reaction (PCR), and behavioral assays, 6-wk-old, male C57BL/6 mice were obtained from Jackson Laboratory (Bar Harbor, ME, USA). Additionally, male CX3CR1-GFP (B6.129P-Cx3cr1tm1Litt/J) mice were also obtained from Jackson Laboratory to analyze glial activation in the NAc. All animals were housed on a 12-h light–dark cycle with unlimited access to water and standard calorie chow. After arriving at the University Laboratory Animal Research (ULAR) facility, animals were group housed for the first 48 h, then separated and housed individually for 24 h prior to the induction of CCI injury. The Institutional Animal Care and Use Committee at Temple University (Philadelphia, PA, USA) approved all procedures involving the use of vertebrate animals.

Controlled Cortical Impact

Animals were prepared for surgery as previously described.[4] Briefly, animals were weighed and anesthetized using 100/10 mg/kg ketamine/xylazine (Henry Schein Animal Health, Dublin, OH, USA) administered via intraperitoneal (ip) injection. Depth of anesthesia was monitored by hind paw toe pinches to assure animals remained sedated during surgical procedures. Once anesthetized, fur was removed surrounding the surgical site using a cordless trimmer (Harvard Apparatus, Holliston, MA, USA). Animals were immobilized using a stereotaxic instrument and ophthalmic ointment (Dechra Veterinary Products, Overland Park, KS, USA) was applied to the eyes to prevent drying. The surgical area was cleaned using 70% isopropyl alcohol. Sterile surgical instruments were used to remove the scalp, exposing the skull right of the sagittal suture up to the temporalis muscle and between lambda and bregma. Fascia was removed, and an Ideal Micro-Drill™ (Cell-Point Scientific Inc., Gaithersburg, MD, USA) with a rounded burr (0.5 mm) was used to remove a 4-mm bone fragment exposing the meninges and cortex. To avoid overheating, drill time was minimized, and the skull was periodically rinsed with 1X-PBS. Controlled cortical impact injury was induced using the Impact One™ Stereotaxic instrument (Leica

Microsystems, Buffalo Grove, IL, USA). The impactor piston (2 mm diameter) was positioned and secured over the right parietal lobe contacting the dural surface parallel to the cortical plane. CCI injury was induced along the following parameters: velocity: 4.5 m/s, depth: 2 mm, dwell time: 0.5 s. The site was then covered using a sterile, 5 mm glass coverslip, secured to the skull with Vetbond™ tissue adhesive (3M, St. Paul, MN, USA) to create a waterproof seal at the surgical margins of the scalp. Procedures were performed with the aid of a Zeiss Stemi 2000-C stereomicroscope (Carl Zeiss Microscopy, LLC, Thornwood, NY, USA) outfitted with a SCHOTT EasyLED Ringlight (SCHOTT North America Inc., Elmsford, NY, USA). After surgical procedures, animals were removed from the stereotaxic instrument and returned to their home cage. During the recovery period, an isothermal pad (Braintree Scientific, Inc., Braintree, MA, USA) was used to maintain body temperature. Animals were monitored until regaining consciousness and then inspected daily for 7 d to monitor the surgical site and health of each animal. No craniectomy controls were animals that did not receive a craniectomy or a CCI-TBI. Therefore, the groups used in the study were as follows: no craniectomy/untreated, CCI-TBI/untreated, no craniectomy/dexamethasone, CCI-TBI/dexamethasone. Of note, we did not observe any significant differences between naive and sham animals for either glial activation in the NAc or cocaine CPP.[4] Therefore, since our previous data show similar control end-results for both naive and sham animals, we selected naive (no craniectomy) mice to control for data presented in this study. This was done for 2 reasons: (1) to limit undue animal distress associated with sham surgery and (2) to minimize the number of needed animals whenever possible (as dictated by the guidelines for the ethical use of laboratory animals; i.e., replace, reduce, refine).

Histology and Passive CLARITY Technique

To visualize the extent of cortical damage, brains were harvested from CCI-TBI and no craniectomy control animals 24 h postinjury. First, mice were anesthetized with 2% isoflurane and transcardially perfused using 1X-PBS (Thermo Fisher Scientific Waltham, MA, United States) followed by Poly/LEM fixative (Polysciences, Inc., Warrington, PA). After perfusion, brains were removed from the skull and placed in Poly/LEM fixative for 24 h at 4 °C. Brains were then dissected using an Alto stainless steel brain matrix (CellPoint Scientific Inc.) and coronal segments (2-mm thick) were postfixed in Poly/LEM fixative at 4 °C for an additional 24 h. Next, segments were washed, processed using a Tissue-Tek® VIP® 6 (Sakura Finetek USA, Inc., Torrance, CA), paraffin-embedded using a TN-1500 Embedding Console System (Tanner Scientific, Inc., Sarasota, FL), and sectioned using a rotary microtome (Leica Microsystems Inc.). Sections were then cleared, rehydrated, and stained using SelecTech High Quality Hematoxylin and Eosin Staining System (Leica Biosystems Inc. Buffalo Grove, IL).

To examine glial activation in the NAc, brain tissue was collected for passive clearing and subsequent immunohistochemical staining, as described in Yang et al.[27] First, CX3CR1-GFP mice (B6.129P-Cx3cr1tm1Litt/J) were randomly assigned to the following categories: no craniectomy, acute CCI-TBI, and chronic CCI-TBI ($n = 3$ per condition). After undergoing CCI procedures, animals were sacrificed at either 24 h (acute) or 2 wk (chronic) postinjury. Brains were harvested, fixed, segmented, and washed as described above. Tissue from the region of the NAc was extracted from both ipsilateral and contralateral hemispheres using a 1.25 mm diameter punch-out tool (Stoelting, Wood Dale, IL). In preparation for lipid clearing, NAc punch-outs were infiltrated with liquid hydrogel matrix (4% acrylamide, 0.05% N, N'-methylene bisacrylamide, 0.25% photoinitiator) over the course of 66 h at 4 °C. The hydrogel matrix was then degassed using nitrogen and polymerized in a water bath (37 °C). NAc punch-outs were excised from the hydrogel matrix using a standard scalpel blade and cleared of lipids via incubation in 0.25% SDS, pH 7.5 (prepared in PBS) at 37 °C on an orbital shaker. Within 14 h, punch-outs were cleared. Next, the cleared punch-outs were vigorously washed of residual SDS through 6 changes of PBS over the course of 24 h and then postfixed at room temperature for additional stability prior to immunostaining.

Immunohistochemistry was performed to enhance glial morphology for cytometric analyses. First, NAc punch-outs were coincubated with rabbit anti-mouse ionized calcium-binding adapter molecule 1 (IBA-1) (1:100; Wako Pure Chemical Industries, Ltd, Osaka, Japan) and mouse anti-mouse Glial fibrillary acidic protein (GFAP) (1:100; Cell Signaling Technology, Inc., Danvers, MA) primary antibodies for 3 d at room temperature. Next, punch-outs were gently washed in PBS for 24 h and then coincubated in donkey anti-rabbit Alexa Fluor 488 (1:200; Thermo Fisher Scientific, Inc., Waltham, MA) and donkey anti-mouse Alexa Fluor 594 (1:200; Thermo Fisher Scientific, Inc.) in 2% normal donkey serum for 2 d at room temperature. Finally, punch-outs were gently washed in PBS for 24 h and then mounted upright in a 145 μm cell-imaging dish (Eppendorf AG, Hauppauge, NY) prior to 2-photon and confocal microscopy. Of note, although our representative images depict IBA-1 staining, studies performed in our laboratory reveal similar microglial morphology when capturing CX3CR1-GFP signal from our transgenic mice, however, quenching of the green fluorescent protein (GFP) fluorophore diminished image quality and obscured microglial ramifications in control animals. Therefore, we performed IBA-1 immunostaining so that alterations in microglial morphology could be observed and quantified in the NAc after CCI-TBI.

Microscopy and Image Analysis

Images from paraffin-embedded tissue were acquired using an Eclipse 80*i* microscope (Nikon Instruments, Inc., Melville, NY) outfitted with a DS-Fi2 color camera (Nikon

Instruments, Inc.) and captured using the NIS Elements imaging software (Nikon Instruments, Inc.). Captured images were pseudo-colored using Adobe Photoshop (Adobe Systems Inc., San Jose, CA, USA). In order to visualize glial activation in the NAc, 2-photon and confocal microscopy were performed using a TCS SP5 II MP microscope (Leica Microsystems Inc.) configured with a tunable femtosecond pulsed Mai Tai Ti-Sapphire laser (Spectra-Physics, Santa Clara, CA, USA). A 20X water immersion objective (HCX APO L NA 0.95) was used to visualize each specimen and z-stacks were acquired using LAS imaging software (Leica Microsystems Inc.). To simultaneously acquire representative images of GFAP and IBA-1 immunostaining, 2-photon microscopy was performed using a 779-nm excitation wavelength with 0.5 μm resolution, and fluorescence emission was detected by non-descanned detectors using a FITC-TRITC filter set consisting of a dichroic beamsplitter (BS 560) and 2 bandpass filters (BP 525/50 and BP 585/40). For analysis of microglial cell volume through IBA-1 staining, additional images were acquired by 2-photon microscopy using an 890 nm excitation wavelength with 1.0 μm resolution, and green fluorescence emission was detected using the same detectors and filter settings described above. For all 2-photon imaging sessions, 300 μm z-stacks were obtained at 200 Hz and $1,024 \times 1,024$ pixels per image frame with compensation. In order to analyze astrocyte activation through the intensity of GFAP immunostaining, confocal microscopy was performed using the same step size, frequency, pixel size, and xyz coordinates imaged during 2-photon sessions. Confocal images were acquired using internal detectors, and a 561-laser line with compensation. All z-stacks (confocal and 2-photon) were merged and analyzed using Imaris 8.1.2 (Bitplane AG, Concord, MA, USA). The Imaris surface module was used to determine average microglia cell volume per region of interest (ROI) per z-stack. Objects were identified with surface area detail of 0.1 μm and an absolute threshold intensity of 25.0. Results were filtered to exclude objects with surface area below 50.0 μm^2 and volumes above 5,000 μm^3, as these values can represent cell fragments or clusters of cells detected as a single object. Results are presented as mean volume (μm^3) (SD). The Imaris surface module was further utilized to determine intensity mean for GFAP staining within the same ROIs per z-stack. Intensity mean statistics describe fluorescence intensity of voxels enclosed within a contour surface. For intensity mean, parameters were as follows: surface area detail 1 μm, absolute threshold intensity 18.0, no filtering.

Dexamethasone Dosage Regimen

A dexamethasone dosage regimen was prepared in consultation with a veterinary postdoc in the Department of Pathology and Laboratory Medicine at Temple University. Dexamethasone was administered by ip injection beginning 24 h after the induction of CCI injury. Deescalating maintenance doses of dexamethasone were then administered every 48 h. The following dosage regimen was used: 4 mg/kg, 24 h postinjury (day 2); 2 mg/kg, 72 h postinjury (day 4); 1 mg/kg, 120 h postinjury (day 6); and 0.5 mg/kg, 168 h postinjury (day 8). Dexamethasone was administered to no craniectomy controls at the same time as CCI-TBI animals using the same dosage schedule described above.

Locomotor Activity Monitoring

One week after the induction of experimental TBI, animals entering the CPP assay were evaluated for locomotor deficits. Prior to activity monitoring, animals were acclimated to the behavioral testing room for 30 min. Animals were then placed in an open field ($18'' \times 14'' \times 8''$), and locomotor activity was monitored using the AccuScan Home Cage Activity System (Omnitech Electronics, Inc., Columbus, OH, USA) for 30 min. Fusion Software (Omnitech Electronics, Inc.) was used to collect data from sensor panels that monitor a set of 16 photobeams arranged along the horizontal axis of the testing chamber. Data were collected in 5-min intervals over the 30-min testing session. Ambulatory activity counts and stereotypy activity counts are recorded as part of the AccuScan Home Cage System variables, and the combination of these 2 counts represent total locomotor activity. Ambulatory activity counts represent the number of photobeam brakes detected by the sensor panel as an animal moves horizontally in the open field. Stereotypy activity counts represent the number of photobeam interruptions occurring repeatedly at a single photobeam and identifies all nonambulatory activity in the open field but does not distinguish between types of stereotypy (i.e., head bobbing or grooming). Any CCI-TBI animal exhibiting locomotor deficits greater than 1½ times standard deviation from the mean cumulative total activity of no craniectomy controls was excluded from the CPP assay. At the end of activity monitoring, animals were removed from the open field and returned to their home cages in ULAR facilities.

Conditioned Place Preference

As previously described, a biased CPP assay consisting of 3-phases was used to assess preference for a cocaine-paired environment.[4] The CPP assay was performed using chambers (approximately $13.75''L \times 5.25''W \times 5.00''H$) divided into 2, equal-sized compartments: one outfitted with black walls and a grit-textured floor, and the other with white and black striped walls and a smooth-textured floor. During phase 1 (day 15 postinjury), a 30-min pretest was analyzed to establish compartment bias by allowing animals to move freely between the 2 compartments through an opening in the divider wall. Preferred compartments were assigned by identifying greater than 15 min residence time (over 50% of the total test) in a single compartment. During phase 2, animals were confined to their nonpreferred compartment for 30 min immediately after receiving an ip injection of cocaine (10 mg/kg dissolved in 0.9% sterile saline) each morning for

6 consecutive days (days 16–21 postinjury). During these sessions, control animals received an equal volume of sterile saline. Four hours later, all animals were immediately confined to their preferred compartment for 30 min after receiving an ip injection of 0.9% sterile saline (equal to the volume administered in the morning). Phase 3 (day 22 postinjury) consisted of a 30-min posttest during which animals were again permitted to move freely between the 2 compartments. In order to calculate place preference shifts, the residence time in the nonpreferred compartment during the pretest was subtracted from the residence time in the nonpreferred (drug-paired) compartment during the posttest. When performing statistical analysis, animals producing shift values less than 90 s or greater than 500 s were excluded from the study to account for behavior not evoked by cocaine conditioning. After each testing session, animals were removed from the CPP chamber and placed in their home cages.

Real-Time PCR

The ipsilateral NAc was isolated from CCI-TBI animals receiving dexamethasone therapy and untreated controls ($n = 3$ per group) at 1 wk (last day of dexamethasone dosage regimen) and 2 wk postinjury (beginning of cocaine CPP). First, mice were transcardially perfused with PBS. Brains were then removed and coronal segments containing the NAc were submerged in RNA*later*® (Thermo Fisher Scientific, Inc.) following vendor instructions. Next, the ipsilateral region of the NAc was excised from each segment using a 1.25-mm diameter punch-out tool (Stoelting Co.), and total RNA was extracted from the tissue using TRIzol® Reagent (Thermo Fisher Scientific, Inc.). RNA concentrations for each sample were quantified using a NanoDrop 1000 Spectrophotometer (Thermo Fisher Scientific, Inc.). To prepare complementary DNA (cDNA), an Eppendorf Mastercycler® pro (Eppendorf AG) and a high-capacity cDNA reverse transcriptase kit (Thermo Fisher Scientific, Inc.) were utilized. TaqMan® Fast Universal PCR Master Mix (Thermo Fisher Scientific, Inc.), nuclease free water, and cDNA were combined with probes for the following targets for mouse: CCL2, CD163, CXCL10, CXCL12, ICAM-1, IL-5, NUR77 (nerve growth factor IB or NR4A1), SELE, TLR4, and eukaryotic 18S (Thermo Fisher Scientific, Inc.). Samples were analyzed using the ΔΔCt method (relative quantification) with a StepOnePlus™ Real-Time PCR System (Applied Biosystems, Inc., Waltham, MA, USA). Data are expressed as the relative fold change + Standard Error Mean (SEM) of no craniectomy controls.

Flow Cytometry

No craniectomy controls and CCI-TBI animals were sacrificed after the last injection of dexamethasone (day 8 postinjury). Untreated controls (both no craniectomy and CCI-TBI animals) were sacrificed at the same time. Blood samples were collected from the posterior vena cava in

EDTA-coated tubes. Total blood cells were isolated from plasma by centrifugation (1,200× g, 5 min, 4 °C). Red blood cells were then lysed using 1X-RBC lysis buffer following the manufacturer's instructions (Affirmetrix, Santa Clara, CA, USA). Next, samples were washed and resuspended in 100 μL flow cytometry buffer (Affirmetrix). Each sample was then incubated for 15 min on ice with purified rat anti-mouse CD16/CD32 antibody (Mouse BD Fc Block™; BD Biosciences, San Jose, CA, USA). Cells were then washed and labeled at 4 °C for 40 min with the following antibodies: FITC-CD45, Pacific Blue-CD11b, APC-CD115, PE-Ly6C, PerCP-5.5-LY6G, fixable viability dye, eFluor® 780. All antibodies were purchased from Affirmetrix unless indicated otherwise. Fluorescent-activated cell sorting (FACS) and data acquisition were performed using a BD FACS Canto II and the BD FACSDiva software (BD Biosciences), respectively. 10,000 events were acquired for each sample and results were analyzed with FlowJo software (Tree Star, Ashland, OR, USA).

Statistical Analysis

Prism 6 (GraphPad Software, Inc., La Jolla, CA, USA) was used to calculate statistical significance: $P \leq .05$. Student *t* tests were performed to analyze real-time PCR and microscopy data. Flow cytometry, activity monitoring, and CPP assays were analyzed by 2-way analysis of variance (ANOVA) with Tukey or Sidak post hoc tests.

Results

Deep Tissue Imaging Reveals Activated Glial Morphology in the NAc Following CCI-TBI in the Adolescent Brain

Figure 1a depicts gross cortical damage sustained by moderate CCI-TBI animals 24 h postinjury. This degree of brain injury typically results in the transcriptional upregulation of IBA-1 and GFAP, as well as the formation of a glial scar consisting of astrocytes with hypertrophic processes and microglia with amoeboid morphology at the site of injury.[4,28–30] Although glial activation at the site of injury is routinely reported following experimental TBI, few studies have assessed changes in glial morphology at the ventral striatum, where structures such as the NAc are located, following a TBI event.

In order to visualize morphological changes in glial cells in the NAc, 2-photon microscopy imaging utilizing tissue clearing techniques was employed. Deep tissue imaging offers the ability to evaluate, in fine detail, the spatial distribution of glial cells, complexity of their processes, and morphological status. Large z-section scans were rendered into 3D volumetric data and processed into isometric views in order to measure microglial volume and the intensity of astrocytic GFAP expression. Representative images from a no craniectomy control reveal the basal expression of GFAP in astrocytes and of IBA-1 in microglia in the NAc (Fig. 1b).
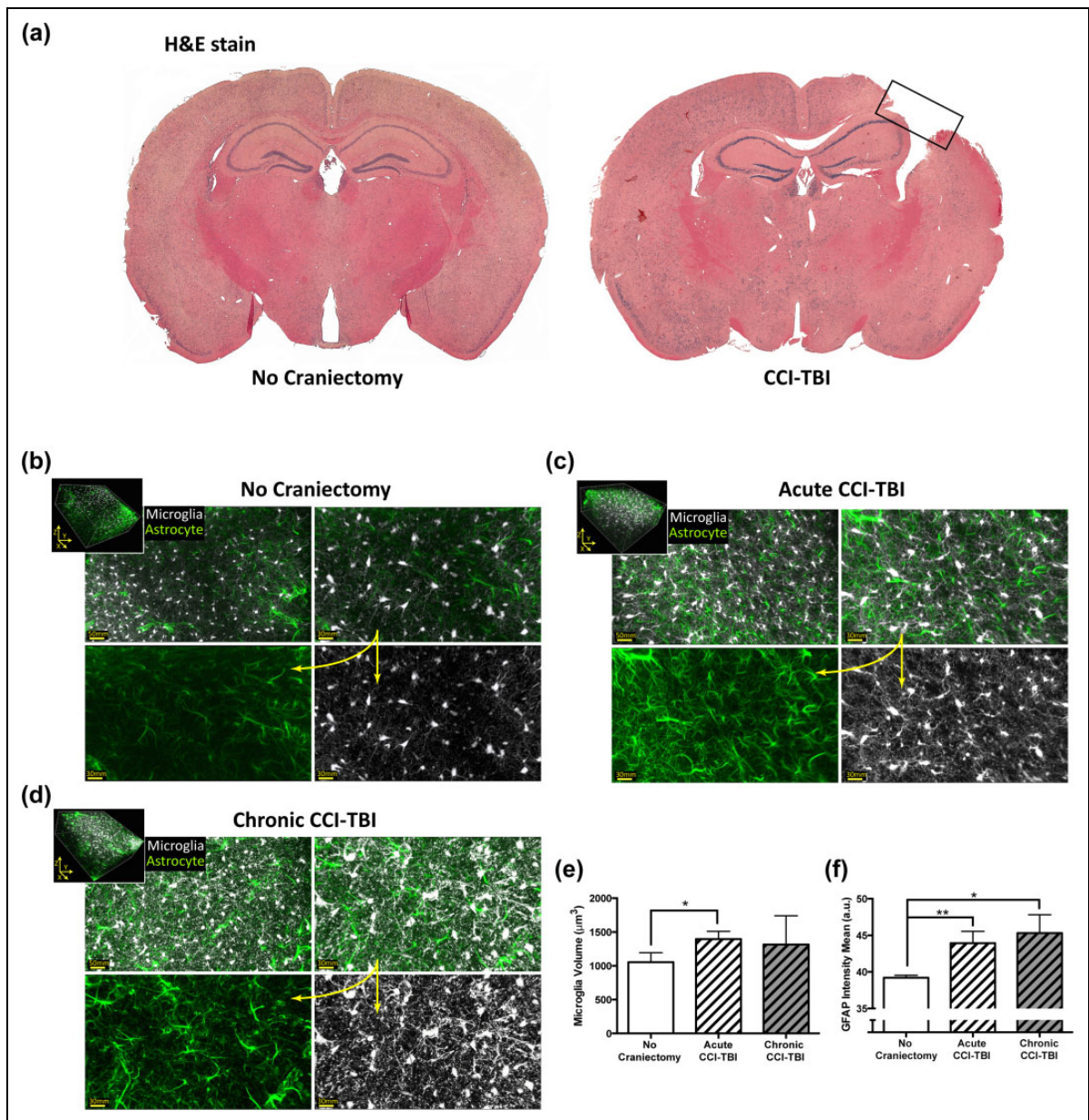
Figure 1. Magnitude of cerebral damage following controlled cortical impact (CCI) injury and analysis of glial morphology and activation status in the nucleus accumbens (NAc) at acute and chronic time points following CCI-traumatic brain injury (TBI). (a) Six-week-old adolescent male C57BL/6 mice underwent moderate CCI-TBI as described in Materials and Methods. Brains were harvested 24 h after CCI-TBI, processed, sectioned, and stained with hematoxylin & eosin. Rectangular box indicates site of cortical injury (right parietal somatosensory cortex) in CCI-TBI animals. (b-f) Using a passive CLARITY technique, immunofluorescence, and 2-Photon microscopy, microglial and astrocyte morphology were analyzed in the NAc of CCI-TBI mice at 24 h (acute) and 2 wk (chronic) postinjury. Brains were sectioned into 2-mm thick segments and the NAc was extracted using a 1.25-mm microdissection tool. (b) Representative images of immunostained IBA-1 positive microglia (pseudocolored silver-white) and GFAP positive astrocytes (pseudocolored emerald-green) in the ipsilateral NAc of a noncraniectomized control animal. Top panels display increasing magnification (scale bars 50 and 30 microns). Bottom panels show unmerged images at higher power (scale bar 30 microns). (c and d) Representative images of changes in microglial morphology and astrocyte GFAP expression can be seen for acute (c) and chronic (d) CCI-TBI groups. (b-d) Insets show representative 300μm z-stacks (3-dimensional volumetric renderings of IBA-1 and GFAP immunostaining) analyzed for microglial volume and GFAP fluorescence intensity. (e) Quantitative morphometric analysis of microglial cell volume in experimental animals ($n = 3$ per group) for objects with volumes determined to be less than 5000 μm^3. (f) Analysis of intensity mean for astrocytic GFAP signal detection in CCI-TBI animals and experimental controls ($n = 3$ per group). Data presented as mean (SD, standard deviation). *$P <.05$. **$P < .01$.

In control animals, astrocytes (pseudocolored emerald-green) have a stellate appearance and thin processes, while microglia (pseudocolored silver-white) have small cell bodies and long fine ramifications. Acutely, 24 h after injury (Fig. 1c), glial activation can be observed in the ipsilateral NAc by upregulation of GFAP and IBA-1. Glial activation
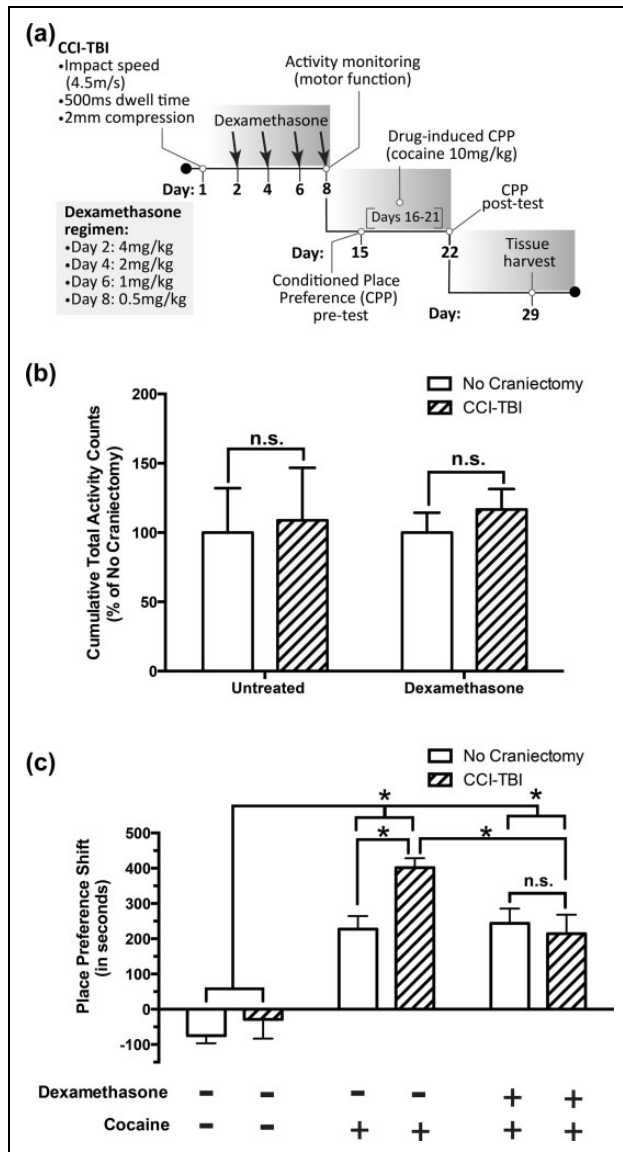
Figure 2. Anti-inflammatory dexamethasone treatment following adolescent controlled cortical impact (CCI)-traumatic brain injury (TBI) blocks significant increases in the cocaine place preference of untreated CCI-TBI controls without producing protracted aversion. Adolescent (6-wk-old), male C57BL/6 mice sustaining moderate CCI-TBI and no craniectomy controls were randomly assigned into dexamethasone or untreated control groups. At the end of dexamethasone treatment (day 8 postinjury), an activity monitoring assay was used to assess potential locomotor impairment arising as a result of either CCI procedures or dexamethasone administration. (a) A schematic model of experimental time points detailing moderate CCI injury parameters, dexamethasone dosage regimen, and schedule of behavioral assays post-TBI. (b) Cumulative total activity (a combination of ambulatory and stereotypy activity counts) recorded during a 30-min test session. Results are presented as mean percent of no craniectomy controls + standard error of mean (SEM). Data were analyzed by 2-way analysis of variance (ANOVA) with Tukey post hoc tests. ns (no significance); $P > .05$. (c) Animals without locomotor deficits proceeded to a 3-phase conditioned place preference assay beginning on day 15 postinjury (1 wk after the last injection of dexamethasone). Animals

was detectable in the NAc after CCI-TBI by the appearance of hypertrophic astrocytic processes and larger microglial cell bodies (Fig. 1c). Notably, these phenotypic changes are sustained chronically, as Fig. 1d shows that astrocyte and microglial activation status in the ipsilateral NAc 2 wk post-TBI is greatly different from basal conditions observed in the no craniectomy controls (Fig. 1b).

Figure 1e shows quantification of microglial volume (μm^3; based on IBA-1 immunostaining). Particle analysis and thresholding based on volume parameters showed a significant increase in microglial volume compared to no craniectomy controls in the ipsilateral NAc 24 h post-TBI (Fig. 1e). Analysis based on GFAP fluorescence signal intensity from astrocytes revealed significantly greater GFAP signal intensity from immunopositive astrocytes following CCI-TBI at both acute and chronic time points when compared to control (Fig. 1f). Together these data reveal that glial activation is present in the NAc post-TBI.

Dexamethasone Normalizes Enhancement in the Rewarding Effects of Cocaine Following Adolescent CCI-TBI

Our previous work demonstrated that the reinforcing effects of the psychostimulant cocaine are increased in adolescent animals that had experienced TBI compared to animals without injury. As shown in Fig. 1, CCI-TBI triggers inflammatory responses that can affect the ventral striatum. Therefore, we hypothesized that by inhibiting inflammatory responses in the acute phase of TBI, that normalization or a return to baseline in the response to the psychostimulant could be achieved. To test this notion, the efficacy of the anti-inflammatory steroidal compound, dexamethasone, was used to evaluate whether dexamethasone treatment could prevent the increases in the rewarding effects of cocaine displayed by animals sustaining moderate CCI-TBI during adolescence.

A dosage regimen was designed that entailed starting with a high-dose (4 mg/kg) injection of dexamethasone at 24 h postinjury (Fig. 2a), as this dose has previously been shown to prevent immune cell accumulation in the brain.[31] In order to avoid potential adverse effects associated with dexamethasone-induced suppression of hypothalamic-pituitary-adrenal axis function in experimental animals, dexamethasone injections were only administered every 48 h

Figure 2. (continued) were conditioned using an optimal dose of cocaine (10 mg/kg) for 6 consecutive days. Place preference shifts were calculated by subtracting residence time in the cocaine-paired environment during the pretest from residence time in the cocaine-paired environment during the posttest. Animals receiving saline only (no dexamethasone treatment, no cocaine) were used as assay controls. Data are presented as mean place preference shift (in seconds) + SEM and were analyzed by 2-way ANOVA with Tukey and Sidak post hoc tests. *$P < .05$. ns (no significance); $P > .05$.

and in deescalating maintenance doses as presented in Fig. 2a. Furthermore, no craniectomy/dexamethasone controls received equivalent doses of dexamethasone at the same time as CCI-TBI animals.

Prior to the CPP assay, mice were evaluated for locomotor deficits. These experiments were performed to ensure that CCI-TBI animals were able to explore the CPP chamber as well as no craniectomy controls and thus should not confound results of the CPP assay. One week after CCI-TBI, total locomotor activity was assessed over a 30-min period (Fig. 2b) and showed no significant locomotor deficits in CCI-TBI animals compared to no craniectomy controls. Therefore, comparisons made in the CPP assay should not be affected by reduced exploratory behavior stemming from locomotor impairment related to CCI injury.

Regarding cocaine-induced CPP, as expected, all animals administered cocaine displayed significant place preference shifts compared to saline controls (no craniectomy and CCI-TBI animals receiving neither cocaine nor dexamethasone; Fig. 2c). Furthermore, in animals receiving cocaine only (no dexamethasone treatment), a significant increase in the cocaine-induced place preference shift of CCI-TBI animals compared to no craniectomy controls (Fig. 2c) was observed. However, in CCI-TBI/dexamethasone animals, no significant increase in cocaine place preference was recorded compared to no craniectomy/dexamethasone controls (Fig. 2c). Furthermore, no craniectomy/dexamethasone animals exhibited place preference shifts similar to no craniectomy controls receiving cocaine only (Fig. 2c). Together, these results demonstrate that dexamethasone treatment immediately following moderate CCI-TBI can block the aberrant increases in the cocaine place preference of CCI-TBI animals.

Dexamethasone Significantly Reduces the Induction of select Immune Response Genes in the NAc in CCI-TBI Animals

After observing a significant reduction in the cocaine place preference shift of CCI-TBI/dexamethasone animals compared to CCI-TBI/untreated animals, we investigated the anti-inflammatory activity of dexamethasone in the NAc by evaluating the relative expression of specific immune response genes. Tissue was harvested 1 or 2 wk post-TBI, which coincides with the end of dexamethasone treatment and the beginning of cocaine CPP, respectively. No craniectomy controls were sacrificed at the same time as CCI-TBI animals and used for relative quantification of gene expression in the NAc by real-time PCR. Gene expression at both 1 and 2 wk post-TBI is normalized to the housekeeping gene, 18S, and presented as fold change from no craniectomy controls (Fig. 3).

At 1 postinjury CCI-TBI/untreated animals show significant increases in the expression of CD163 in the NAc (Fig. 3a and b). CD163 is a known marker for activated microglia, which is elevated at 1 wk post-TBI.[32] Furthermore, results
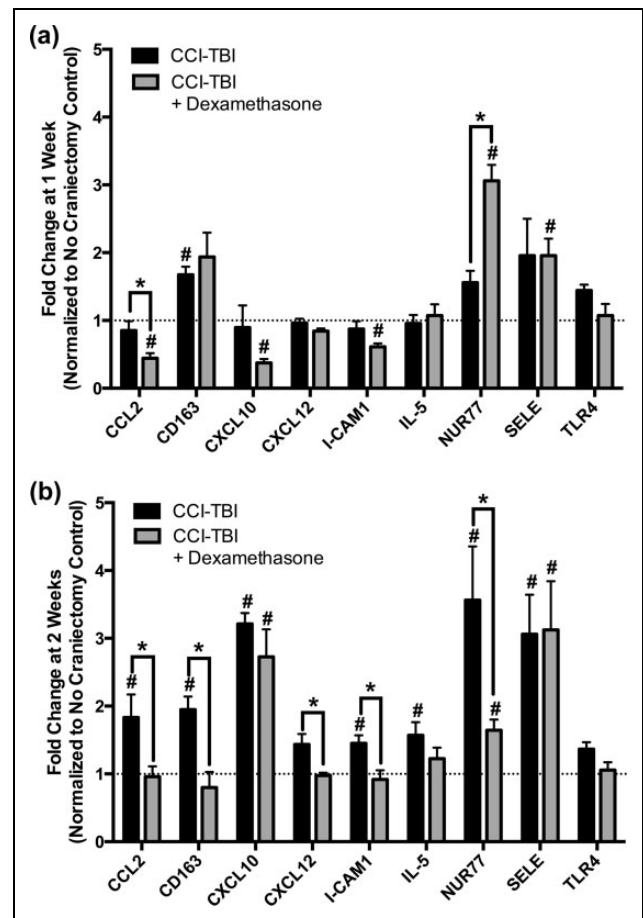
Figure 3. Dexamethasone significantly alters the expression of select immune response genes in the nucleus accumbens (NAc) after controlled cortical impact (CCI)-traumatic brain injury (TBI). The ipsilateral NAc was extracted from CCI-TBI animals (dexamethasone and untreated controls) at 1 wk (end of dexamethasone injections) and 2 wk postinjury (immediately prior to cocaine conditioning). Total RNA was isolated, converted to complementary DNA (cDNA), and analyzed for expression of the following mouse genes by real-time polymerase chain reaction (PCR): *CCL2, CD163, CXCL10, CXCL12, ICAM-1, IL-5*, nerve growth factor IB (*Nur77*), Selectin E (*SELE*), *TLR4*, and housekeeping, eukaryotic 18S. Data were analyzed by $\Delta\Delta Ct$, normalized to 18S, and are expressed as mean fold change from no craniectomy controls + standard error of the mean (SEM) (a) Fold change of immune response genes 1 wk post CCI-TBI. Statistical significance was determined by Student t test. #$P < .05$ compared to no craniectomy controls. *$P < .05$ between CCI-TBI and CCI-TBI/dexamethasone animals. (b) Fold change of immune response genes 2 wk post-CCI. Statistical significance was determined by Student t test. #$P < .05$ compared to no craniectomy controls. *$P < .05$ between CCI-TBI and CCI-TBI/dexamethasone animals.

presented in Fig. 3b identified the upregulation of immune response genes (*CCL2, CXCL10, ICAM-1*, and *SELE*) in the NAc at 2 wk post-CCI. Interestingly, target gene CD163 remained significantly overexpressed in the NAc of CCI-TBI/untreated animals at 2 wk compared to no craniectomy controls. In addition, NUR77, a transcription factor expressed by nonclassical or patrolling monocytes, was significantly elevated in CCI-TBI/untreated animals at 2 wk

when compared to no craniectomy controls, suggesting an immune cell-mediated response to the injuries in the NAc post-TBI (Fig. 3b).

A much different response was observed in CCI-TBI/dexamethasone animals. One week after CCI-TBI (immediately after the final injection of dexamethasone; day 8 postinjury, see Fig. 2a), select immune response genes, namely, *CCL2*, *CXCL10*, and *ICAM-1*, were significantly down regulated in the NAc of CCI-TBI mice compared to no craniectomy controls (Fig. 3a). Then 2 wk after CCI-TBI, expression of CCL2 and ICAM-1 returned to control levels, and CXCL10 became significantly overexpressed (Fig. 3b). Moreover, 2 genes, *Nur77* and *SELE*, were significantly overexpressed in the NAc of CCI-TBI mice at both 1 and 2 wk post-CCI when compared to no craniectomy controls (Fig. 3a and b). Interestingly, significant differences in the expression of immune response genes were also identified between CCI-TBI/dexamethasone and CCI-TBI/untreated animals at both 1 and 2 wk postinjury. First, at 1 wk, CCI-TBI/dexamethasone animals expressed significantly greater levels of *Nur77*, whereas expression of *CCL2* was significantly lower compared to CCI-TBI/untreated group (Fig. 3a). Furthermore, at 2 wk postinjury, a significant decrease in the expression of *CCL2* held in CCI-TBI/dexamethasone animals compared to CCI-TBI/untreated, along with significant reductions in the expression of *CD163*, *CXCL12*, *ICAM-1*, and *Nur77*. Of note, although multiple reports have implicated TLR4 as a mediator of drug abuse behavior, our data revealed no significant changes in TLR4 expression in the NAc at either 1 or 2 wk as a result of CCI-TBI or dexamethasone administration (Fig. 3a and b). The analysis from these studies clearly point to temporal inflammatory responses in the NAc after injury. Consequently, the anti-inflammatory outcomes of dexamethasone treatment on the NAc are evident by the downregulation of key inflammatory genes.

## Dexamethasone Induces an Anti-Inflammatory Phenotypic Change in Monocyte Populations

Given the results of our gene expression analyses, which show significant changes in the expression of chemokines, cell adhesion molecules, transcription factors, and markers of immune cell activation in the NAc as a result of dexamethasone administration, a closer look was taken to evaluate the effect of dexamethasone on peripheral blood leukocyte populations, specifically focusing on monocyte subtypes, following CCI-TBI. To characterize monocytes in the bloodstream, blood was collected and analyzed at 1 wk from the following group of animals no craniectomy/untreated, CCI-TBI/untreated, no craniectomy/dexamethasone, and CCI-TBI/dexamethasone. Monocytes were identified based on expression of $CD45^+$/$CD11b^+$/$Ly6G^-$/$CD115^+$ and monocyte subtypes were gated on differential Ly6C expression (Fig. 4a). The percentage of monocytes (out of $CD45^+$ cells) was unchanged between all conditions except for CCI-TBI/dexamethasone, which had a significant

reduction (by ⅓) in total monocytes compared to both untreated conditions (Fig. 4e). To determine whether the change in total monocytes was due to a reduction in a specific monocyte subtype, the percentage of each subtype was plotted (Fig. 4g). Overall, CCI-TBI did not have any significant effect while dexamethasone treatment induced clear changes in the percentage of some monocyte subtypes. Specifically, dexamethasone treatment equally reduced the percentage of $Ly6C^{hi}$ inflammatory monocytes by ½ for both the no craniectomy and CCI-TBI conditions (Fig. 4g, left). The percentage of $Ly6C^{med}$ did not change significantly between any of the groups (Fig. 4g, middle). $Ly6C^{lo}$ nonclassical or patrolling monocytes showed differential changes with dexamethasone treatment between no craniectomy and CCI-TBI. Dexamethasone alone elevated the percentage of $Ly6C^{lo}$ monocytes by ⅓ while combined with CCI-TBI $Ly6C^{lo}$ monocytes were decreased by ¼ compared to the no craniectomy/untreated, suggesting the loss in the percentage of monocytes was mainly due to a reduction in this subtype in circulation.

Dexamethasone has been reported to alter monocyte phenotypes in both humans and mice.[33,34] To determine whether our conditions induced changes in monocyte subtypes, Ly6C expression was analyzed. Representative contour plots for each of the conditions (Fig. 4a-d) show a clear change in both dexamethasone conditions. The results show that the contour plots are similar between no craniectomy/untreated (Fig. 4a) and CCI-TBI/untreated (Fig. 4c), and between no craniectomy/dexamethasone (Fig. 4b) and CCI-TBI/dexamethasone (Fig. 4d). Bar graph representation of the 3 subtypes together shows a similar shift as a result of dexamethasone treatment (Fig. 4f). The percentage of each subtype was plotted separately to best show the changes between the groups (Fig. 4g). CCI-TBI alone did not have any significant effect on any percentages of the monocyte subtypes. However, dexamethasone treatment resulted in a significant decrease of 65% to 70% in the percentage of $Ly6C^{hi}$ classical monocytes and a significant increase of 40% to 45% in $Ly6C^{med}$ intermediate monocytes in both the no craniectomy and CCI-TBI conditions. In addition, dexamethasone statistically increased the percentage of $Ly6C^{lo}$ by 40% of nonclassical monocytes in the no craniectomy condition compared to both CCI-TBI conditions. This shift resulting from dexamethasone treatment was not as large in the CCI-TBI condition (an increase of 15%), presumably due to the extravasation of this subtype into the tissue. Together these results provide evidence for a shift in monocyte subtype toward a more anti-inflammatory phenotype due to dexamethasone treatment. In addition, the increase in circulating patrolling monocytes allows the immune system to rapidly respond and induce extravasation of the $Ly6C^{lo}$ nonclassical monocyte to the damaged areas.

Discussion

In this report, we test the hypothesis that enhancement of the rewarding effects of cocaine displayed by CCI-TBI animals
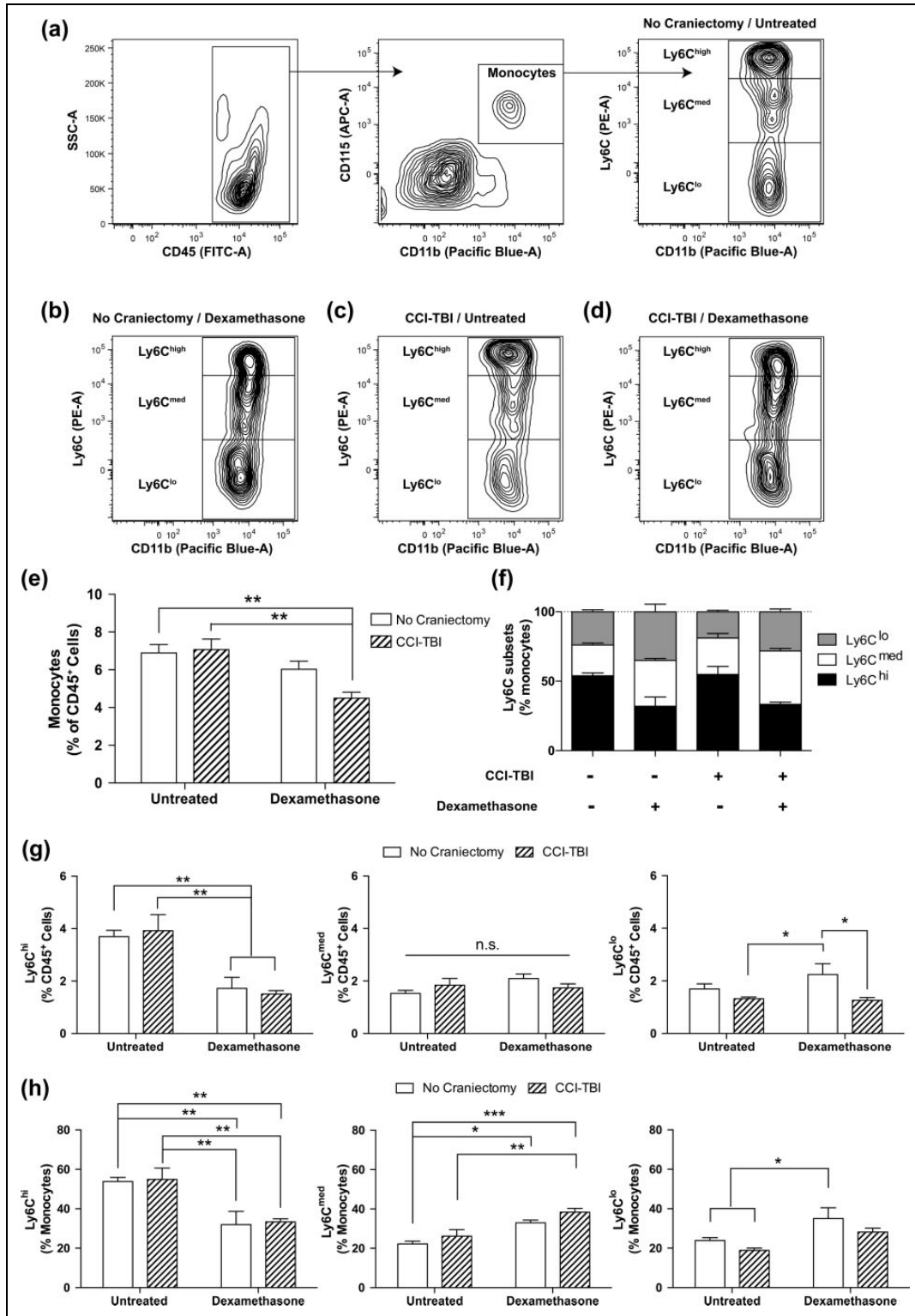
Figure 4. Dexamethasone treatment shifts monocyte populations to noninflammatory phenotype. Monocyte phenotype was assessed at 1-wk post-traumatic brain injury (TBI) in mice treated with or without dexamethasone. (a-d) Representative Fluorescence-activated cell sorting (FACS) contour plots of monocyte gating (CD45+/CD11b+/Ly6G-/CD115+). Gates are shown by the solid line. Monocyte phenotype was then determined by differential Ly6C expression (hi, med, lo) and shown for no craniectomy/untreated (a), no craniectomy/dexamethasone (b), controlled cortical impact (CCI)-TBI/untreated (c), and CCI-TBI/dexamethasone (d). (e) Bar graph plotting monocytes as a percentage of CD45+ cells for each condition. Two-way analysis of variance (ANOVA) and Tukey post hoc test, **$P < .01$. (f) Frequency of monocyte phenotype Ly6C subpopulations for each of the conditions listed above. (g) Ly6C subtypes as a percentage of CD45+ cells for each condition were plotted. Two-way ANOVA and Tukey post hoc test, *$P < 0.05$, **$P < .01$. (h) Ly6C subtypes were plotted as a percentage of monocytes. Two-way ANOVA and Tukey post hoc tests, *$P < .05$, **$P < .01$.

is a function of chronic neuroinflammation in the NAc, as recent reports suggest immune signaling can potentiate drug and alcohol abuse behavior.[7–12,35] In order to test this hypothesis, we administered a synthetic, anti-inflammatory corticosteroid (dexamethasone) therapy beginning 24 h post CCI-TBI (Fig. 2a). Results of these studies showed a significant decrease in the cocaine place preference (CPP) shift of CCI-TBI/dexamethasone mice compared to CCI-TBI/ untreated animals, and a return to no craniectomy control behavior in response to cocaine conditioning (Fig. 2c). Importantly, the return to the "normal" cocaine-induced CPP promoted by dexamethasone could be attributed to the effects of dexamethasone in attenuating inflammatory responses in the NAc. Interestingly, our findings also indicate the possible involvement of patrolling monocytes in the resolution of inflammation in this critical area of the reward pathway.

We began evaluating injury in the NAc after experimental TBI in order to understand how damage in this brain nucleus may influence behavior toward illicit drugs of abuse. Following our recent publication,[4] we now present the first volumetric analysis of NAc after experimental TBI, showing both astrocyte and microglial activation (Fig. 1b and c) and the upregulation of numerous immune response genes post-injury (Fig. 3). Our studies are in agreement with other investigations where the presence of increased reactive astrocytes (evaluated by elevated GFAP expression) can be seen in the NAc in both blast and closed head injury models of TBI.[36,37] These studies have also identified upregulation of apoptotic markers in the NAc, suggesting that TBI may cause neuronal cell death in regions of the brain that mediate drug abuse behavior.[37] Furthermore, recent investigations have identified neuroradiological abnormalities in the NAc of patients with a history of TBI when compared to uninjured control subjects.[38,39] Interestingly, these abnormalities have been shown to strongly correlate with neuropsychiatric impairment and longer recovery time postinjury.[39]

Consistent with our previous study, we delayed beginning the CPP assay until 2 wk post-TBI, as clinical reports indicate an upward trend in substance abuse among TBI patients as time increases postinjury.[40] Furthermore, we purposefully set out with the intention of testing the effect of adolescent CCI-TBI on the development and expression of addiction-like behavior later in early adulthood. Notably, according to the National Survey on Drug Use and Health, this transitional period (adolescence to early adulthood) marks the greatest increase in illicit drug use among the general population over the age of 12.[41] Thus, the 2-wk delay also permitted adolescent animals to mature to an age developmentally comparable to early adulthood allowing us to appropriately model and test our hypothesis. As our goal was to block the significant enhancement in cocaine place preference exhibited by moderate CCI-TBI mice compared to controls, not completely block the rewarding effects of cocaine in both CCI-TBI and control animals, we paired our dexamethasone treatment with the subacute phase

immediately following CCI-TBI (with the intention of suppressing immune activation related to brain injury) rather than undermining the results of our CPP assay by administering dexamethasone too close to or simultaneously with cocaine conditioning.

We selected dexamethasone because of its well-established, potent anti-inflammatory effects. Specifically, in the case of brain trauma sustained during neurosurgical procedures, multiple reports have shown that dexamethasone (administered by either direct intracranial or systemic injection) reduces astrocyte and microglial activation surrounding the site of injury at 1 wk.[42–47] These anti-inflammatory effects have still been observed up to 6 wk postinjury, suggesting stable glial suppression may be achieved with dexamethasone treatment following experimental brain injury. Furthermore, in accordance with studies showing that dexamethasone suppresses CCL2 expression via a mitogen-activated protein kinase phosphatase-1 dependent mechanism in rat microglia, we observed significant reductions in CCL2 expression at both 1 and 2 wk post-CCI (Fig. 3).[48] Of note, additional studies have shown that dexamethasone attenuates neuronal loss and equilibrates dopamine and glutamate transmission surrounding the site of injury.[45,47,49] These effects are noteworthy, as both TBI and drug abuse are known to impair dopaminergic/glutamatergic transmission and may represent a conserved mechanism of action whereby TBI neurochemically primes the brain for addiction-like behavior. Therefore, through its anti-inflammatory activity, dexamethasone may not only suppress glial activation and the expression of immune response genes but also preserve the function of key neurotransmitter systems affecting drug abuse behavior.

Notably, dexamethasone has also been shown to reduce pathology following experimental TBI.[50–53] These studies have shown that dexamethasone can stabilize blood–brain barrier dysfunction by stimulating glucocorticoid receptor-mediated expression of tight junction proteins.[50] Additional studies have shown that dexamethasone can also reduce cerebral edema following TBI; however, contrary results have also been reported, showing the dexamethasone administration may actually worsen cerebral edema (and other outcomes) post-TBI.[54] Of course, these conflicting results may be a function of the different dexamethasone dosage regimens employed in each study. We designed our dosage schedule beginning with an injection of dexamethasone (4 mg/kg; Fig. 2a) optimal for avoiding the adverse effects associated with high-dose dexamethasone administration, yet potent enough to effectively suppress recruitment and infiltration of circulating immune cells to the brain. Interestingly, although some reports have found that dexamethasone can inhibit recruitment of peripheral blood cells to the brain, others have shown that dexamethasone does not reduce the number of immune cells, specifically mononuclear phagocytes (a.k.a. monocytes), in the brain after TBI, nor impair functions of monocyte/macrophage phagocytosis, astrogliosis, or neovascularization.[55] Furthermore,

these studies have found that monocytes migrate to sites of injury in the brain and play a major role in wound healing during the first week post-TBI, although this may be a function of the monocyte subtype.[55]

Previous terminology regarding monocyte subtype has not been uniform resulting in classical monocytes being labeled as Ly6C^{hi} or Ly6C$^+$ and nonclassical as Ly6C^{lo} or Ly6C$^-$. Consequently, intermediate monocytes, Ly6C^{med} or Ly6C^{int}, have often been inaccurately grouped with either classical Ly6C^{hi} or nonclassical Ly6C$^-$ monocytes. Our gating, which separates each subtype (lo, med, hi) shows baseline levels of the 3 subtypes similar to previous reports[17,56] and highlights clear differential shifts in the 3 subsets as a result of no craniectomy/dexamethasone treatment or CCI-TBI/dexamethasone treatment.

Analysis of the percentage of monocytes or monocyte subtype in the blood was unchanged at 1-wk post-TBI (Fig. 4e and h). Previous reports are conflicting with regard to changes in monocyte percentage or subtype at 1-wk post-TBI with some reporting decreases in total monocytes with no changes in Ly6C$^+$ or Ly6C$^-$ cells[25] or increases in Ly6C^{hi} monocytes at 1-wk.[26] These apparent discrepancies may be due to differences in TBI severity and methodology (weight drop vs. CCI, open vs. close head) as well as the different markers used to identify different subsets of peripheral monocytes. Importantly, comparison of our baseline percentages for total monocytes and subtypes was similar to previous reports in C57BL/6J mice[13] using the same markers presented here.

Dexamethasone treatment, which did not have a significant effect on total percentage of monocytes in circulation, induced a clear shift in monocyte phenotype. The reduction in Ly6C^{hi} monocytes (% of total monocytes) was roughly offset by the increase in both Ly6C^{med} and Ly6C^{lo} (Fig. 4h). Whether monocyte differentiation occurs primarily in the blood, bone marrow, or spleen is still a matter of debate[57]; however, one explanation may be that Ly6C^{hi} monocytes differentiate into the other 2 monocyte subtypes as they mature in the blood.[22] Glucocorticoids have been shown to affect cells of the immune system and previous evidence has shown that dexamethasone can shift monocyte phenotype in humans and mice in vitro.[33,34] Varga et al. showed that treatment of murine monocytes with dexamethasone resulted in a distinct phenotype with characteristics in between nonclassical and classical monocytes.[33] While our observation of an overall shift in phenotype is similar to their results, we observed an increase in Ly6C^{lo} that they did not. This may be due to the conditions of the experiment (in vitro vs. in vivo) because monocytes are known to lose their differentiation phenotype under in vitro conditions. Additionally, Varga et al. also used alternative markers for monocytes (CCR2, CX3CR1), which we did not examine.[33] Interestingly, while dexamethasone alone did not result in a decrease in total circulating monocytes, we show a significant decrease in CCI-TBI/dexamethasone treated animals (Fig. 4e). Examination of whether a particular population of

monocytes was responsible for this decrease pointed to a loss of circulating Ly6C^{lo} (Fig. 4g). We believe this is a result in migration of this specific monocyte subtype into the tissue. This is supported by previous reports that show that dexamethasone-treated monocytes migrated more readily through transwell filters[33] and that nonclassical monocytes migrate into the tissue primarily during injury.[58]

The specific importance of nonclassical/patrolling monocytes is still being explored in a number of vascular and neurological diseases. Although not yet investigated in the context of TBI, previous studies examining their importance in atherosclerosis,[56] stroke/ischemia,[14] and excitoxicity[13] may point to the kind of injury following TBI that may benefit from patrolling monocytes. These studies identifying the significance of nonclassical monocytes have primarily used NR4A1$^{-/-}$ mice. NR4A1 (Nur77) is important for the differentiation and survival of nonclassical/patrolling Ly6C^{lo} monocytes.[19] In those studies, the absence of patrolling monocytes leads to worse outcomes in atherosclerosis[56] and sterile excitotoxicity,[13] while no effect was observed following stroke.[14] TBI results in a complex sequence of primary and secondary events and involves many different aspects of the inflammatory response, thus, the role of patrolling monocytes may not be simplistic. It is possible that vascular injury and the type of inflammation present dictate how patrolling monocytes may contribute the resolution of neuroinflammation.

In addition to the decreases in circulating Ly6C^{lo} monocytes, we also examined gene expression of *Nur77*, which is highly expressed in Ly6C^{lo} monocytes, in the NAc.[23] Our results show a dramatic increase in *Nur77* expression at 1 wk post-TBI in dexamethasone-treated animals, which remained elevated at 2 wk (Fig. 3). We have interpreted this increased gene expression of *Nur77* in the NAc as a result increased infiltrated Ly6C^{lo} monocytes or possibly in Ly6C^{lo} differentiated macrophages.[56,59] This concept is supported by recent data showing the importance of patrolling monocytes in M2 macrophage polarization and resolution of inflammation.[56,60] We cannot discount the fact that *Nur77* could be upregulated from alternative cells in the NAc.[61,62] However, *Nur77* is known for its immediate and acute responses to environmental cues, and we show its upregulation at 2 wk (Fig. 3), which is beyond the normal response time and last dose of treatment.[62] Additionally, *Nur77* is upregulated in CCI-TBI/untreated at 2 wk indicating that its presence is not due entirely due to glucocorticoid treatment. We have speculated that this differential time in upregulation of *Nur77* may be a result of a dexamethasone-induced shift in the immune response in repairing the NAc. Aside from being highly expressed in Ly6C^{lo} monocytes, *Nur77* is expressed in endothelial cells during cell proliferation and angiogenesis,[62] however, we do not expect angiogenesis to be occurring in the NAc, given its location away from the site of injury and the time from injury. Therefore, the decrease in the percentage of Ly6C^{lo} monocytes in circulation combined with the increases in *Nur77* gene expression

in the NAc point to an important role for non-classical/patrolling monocytes in reducing TBI-induced behavioral sensitivity to cocaine.

To conclude, our studies found that dexamethasone treatment following CCI-TBI can attenuate the cocaine place preference of injured animals without producing aversion in the CPP assay. This accompanied a reduction in immune response genes, a shift in monocyte phenotype and a reduction in nonclassical patrolling monocytes in circulation. However, it remains to be determined whether both of these effects are required to block enhancement of cocaine reward in CCI-TBI/dexamethasone animals, or if suppressing neuroinflammation alone is sufficient to normalize the response to cocaine following TBI. Overall, our findings indicate that anti-inflammatory agents such as dexamethasone may be effective in normalizing the rewarding effects of cocaine following CCI-TBI.

Authors' Note

Steven F. Merkel and Allison M. Andrews contributed equally to the article.

Ethical Approval

The protocols in this study were approved by the relevant ethics committee (see Materials and Methods).

Statement of Informed Consent

There are no human subjects in this article and informed consent is not applicable.

Declaration of Conflicting Interests

The author(s) declared no potential conflicts of interest with respect to the research, authorship, and/or publication of this article.

Funding

References

1. Whelan-Goodinson R, Ponsford J, Johnston L, Grant F. Psychiatric disorders following traumatic brain injury: their nature and frequency. J Head Trauma Rehabil. 2009;24(5):324–332.

2. Corrigan JD, Bogner J, Mellick D, Bushnik T, Dams-O'Connor K, Hammond FM, Hart T, Kolakowsky-Hayner S. Prior history of traumatic brain injury among persons in the traumatic brain injury model systems national database. Arch Phys Med Rehabil. 2013;94(10):1940–1950.

3. Ramesh D, Keyser-Marcus LA, Ma L, Schmitz JM, Lane SD, Marwitz JH, Kreutzer JS, Moeller FG. Prevalence of traumatic brain injury in cocaine-dependent research volunteers. Am J Addict. 2015;24(4):341–347.

4. Merkel SF, Razmpour R, Lutton EM, Tallarida CS, Heldt NA, Cannella LA, Persidsky Y, Rawls SM, Ramirez SH. Adolescent traumatic brain injury induces chronic mesolimbic neuroinflammation with concurrent enhancement in the rewarding effects of cocaine in mice during adulthood. J Neurotrauma 2017;34(1):165–181.

5. Nestler EJ. Is there a common molecular pathway for addiction? Nat Neurosci. 2005;8(11):1445–1449.

6. Kalivas PW. The glutamate homeostasis hypothesis of addiction. Nat Rev Neurosci. 2009;10(8):561–572.

7. Osterndorff-Kahanek EA, Becker HC, Lopez MF, Farris SP, Tiwari GR, Nunez YO, Harris RA, Mayfield RD. Chronic ethanol exposure produces time- and brain region-dependent changes in gene coexpression networks. PLoS One 2015;10(3):e0121522.

8. Crews FT, Zou J, Qin L. Induction of innate immune genes in brain create the neurobiology of addiction. Brain Behav Immun. 2011;25(Suppl 1):S4–S12.

9. Adler MW, Rogers TJ. Are chemokines the third major system in the brain? J Leukoc Biol. 2005;78(6):1204–1209.

10. Hutchinson MR, Northcutt AL, Hiranita T, Wang X, Lewis SS, Thomas J, van Steeg K, Kopajtic TA, Loram LC, Sfregola C, et al. Opioid activation of toll-like receptor 4 contributes to drug reinforcement. J Neurosci. 2012;32(33):11187–11200.

11. Blednov YA, Benavidez JM, Geil C, Perra S, Morikawa H, Harris RA. Activation of inflammatory signaling by lipopolysaccharide produces a prolonged increase of voluntary alcohol intake in mice. Brain Behav Immun. 2011;25(Suppl 1):S92–S105.

12. Wang X, Loram LC, Ramos K, de Jesus AJ, Thomas J, Cheng K, Reddy A, Somogyi AA, Hutchinson MR, Watkins LR, et al. Morphine activates neuroinflammation in a manner parallel to endotoxin. Proc Natl Acad Sci U S A. 2012;109(16):6325–6330.

13. Bellavance MA, Gosselin D, Yong VW, Stys PK, Rivest S. Patrolling monocytes play a critical role in cx3cr1-mediated neuroprotection during excitotoxicity. Brain Struct Funct. 2015;220(3):1759–1776.

14. Michaud JP, Pimentel-Coelho PM, Tremblay Y, Rivest S. The impact of ly6clow monocytes after cerebral hypoxia-ischemia in adult mice. J Cereb Blood Flow Metab. 2014;34(7):e1–e9.

15. Saber M, Kokiko-Cochran O, Puntambekar SS, Lathia JD, Lamb BT. Triggering receptor expressed on myeloid cells 2 deficiency alters acute macrophage distribution and improves recovery after traumatic brain injury. J Neurotrauma. 2017; 34(2):423–435.

16. Lee J, Costantini TW, D'Mello R, Eliceiri BP, Coimbra R, Bansal V. Altering leukocyte recruitment following traumatic brain injury with ghrelin therapy. J Trauma Acute Care Surg. 2014;77(5):709–715.

17. Yang J, Zhang L, Yu C, Yang XF, Wang H. Monocyte and macrophage differentiation: circulation inflammatory monocyte as biomarker for inflammatory diseases. Biomark Res. 2014;2(1):1.

18. Geissmann F, Jung S, Littman DR. Blood monocytes consist of two principal subsets with distinct migratory properties. Immunity. 2003;19(1):71–82.

19. Carlin LM, Stamatiades EG, Auffray C, Hanna RN, Glover L, Vizcay-Barrena G, Hedrick CC, Cook HT, Diebold S,

Geissmann F. Nr4a1-dependent ly6c(low) monocytes monitor endothelial cells and orchestrate their disposal. Cell. 2013; 153(2):362–375.

20. Gordon S, Taylor PR. Monocyte and macrophage heterogeneity. Nat Rev Immunol. 2005;5(12):953–964.

21. Nahrendorf M, Swirski FK, Aikawa E, Stangenberg L, Wurdinger T, Figueiredo JL, Libby P, Weissleder R, Pittet MJ. The healing myocardium sequentially mobilizes two monocyte subsets with divergent and complementary functions. J Exp Med. 2007;204(12):3037–3047.

22. Thomas G, Tacke R, Hedrick CC, Hanna RN. Nonclassical patrolling monocyte function in the vasculature. Arterioscler Thromb Vasc Biol. 2015;35(6):1306–1316.

23. Hanna RN, Carlin LM, Hubbeling HG, Nackiewicz D, Green AM, Punt JA, Geissmann F, Hedrick CC. The transcription factor nr4a1 (nur77) controls bone marrow differentiation and the survival of ly6c- monocytes. Nat Immunol. 2011;12(8): 778–785.

24. Geissmann F, Auffray C, Palframan R, Wirrig C, Ciocca A, Campisi L, Narni-Mancinelli E, Lauvau G. Blood monocytes: distinct subsets, how they relate to dendritic cells, and their possible roles in the regulation of t-cell responses. Immunol Cell Biol. 2008;86(5):398–408.

25. Schwulst SJ, Trahanas DM, Saber R, Perlman H. Traumatic brain injury-induced alterations in peripheral immunity. J Trauma Acute Care Surg. 2013;75(5):780–788.

26. Lee S, Mattingly A, Lin A, Sacramento J, Mannent L, Castel MN, Canolle B, Delbary-Gossart S, Ferzaz B, Morganti JM, et al. A novel antagonist of p75ntr reduces peripheral expansion and CNS trafficking of pro-inflammatory monocytes and spares function after traumatic brain injury. J Neuroinflammation. 2016;13(1):88.

27. Yang B, Treweek JB, Kulkarni RP, Deverman BE, Chen CK, Lubeck E, Shah S, Cai L, Gradinaru V. Single-cell phenotyping within transparent intact tissue through whole-body clearing. Cell. 2014;158(4):945–958.

28. Burda JE, Bernstein AM, Sofroniew MV. Astrocyte roles in traumatic brain injury. Exp Neurol. 2016;275(Pt 3): 305–315.

29. Mayeux JP, Teng SX, Katz PS, Gilpin NW, Molina PE. Traumatic brain injury induces neuroinflammation and neuronal degeneration that is associated with escalated alcohol self-administration in rats. Behav Brain Res. 2015;279:22–30.

30. Karve IP, Taylor JM, Crack PJ. The contribution of astrocytes and microglia to traumatic brain injury. Br J Pharmacol. 2016; 173(4):692–702.

31. Vachharajani V, Vital S, Russell J, Scott LK, Granger DN. Glucocorticoids inhibit the cerebral microvascular dysfunction associated with sepsis in obese mice. Microcirculation. 2006; 13(6):477–487.

32. Roberts ES, Masliah E, Fox HS. Cd163 identifies a unique population of ramified microglia in hiv encephalitis (hive). J Neuropathol Exp Neurol. 2004;63(12):1255–1264.

33. Varga G, Ehrchen J, Tsianakas A, Tenbrock K, Rattenholl A, Seeliger S, Mack M, Roth J, Sunderkoetter C. Glucocorticoids induce an activated, anti-inflammatory monocyte subset in mice that resembles myeloid-derived suppressor cells. J Leukoc Biol. 2008;84(3):644–650.

34. Ehrchen J, Steinmuller L, Barczyk K, Tenbrock K, Nacken W, Eisenacher M, Nordhues U, Sorg C, Sunderkotter C, Roth J. Glucocorticoids induce differentiation of a specifically activated, anti-inflammatory subtype of human monocytes. Blood. 2007;109(3):1265–1274.

35. Hutchinson MR, Watkins LR. Why is neuroimmunopharmacology crucial for the future of addiction research? Neuropharmacology. 2014;76(Pt B):218–227.

36. Lowing JL, Susick LL, Caruso JP, Provenzano AM, Raghupathi R, Conti AC. Experimental traumatic brain injury alters ethanol consumption and sensitivity. J Neurotrauma. 2014; 31(20):1700–1710.

37. Sajja VS, Galloway M, Ghoddoussi F, Kepsel A, VandeVord P. Effects of blast-induced neurotrauma on the nucleus accumbens. J Neurosci Res. 2013;91(4):593–601.

38. Shah S, Yallampalli R, Merkley TL, McCauley SR, Bigler ED, Macleod M, Chu Z, Li X, Troyanskaya M, Hunter JV, et al. Diffusion tensor imaging and volumetric analysis of the ventral striatum in adults with traumatic brain injury. Brain Inj. 2012; 26(3):201–210.

39. Alhilali LM, Delic JA, Gumus S, Fakhran S. Evaluation of white matter injury patterns underlying neuropsychiatric symptoms after mild traumatic brain injury. Radiology 2015;277(3): 793–800.

40. Parry-Jones BL, Vaughan FL, Miles Cox W. Traumatic brain injury and substance misuse: a systematic review of prevalence and outcomes research (1994-2004). Neuropsychol Rehabil. 2006;16(5):537–560.

41. Administration SAMHS, editor. Results from the 2013 national survey on drug use and health: summary of national findings, NSDUH Series H-48, HHS publication no. (SMA) 14-4863. Rockville (MD): Administration SAMHS; 2014.

42. Kozai TD, Jaquins-Gerstl AS, Vazquez AL, Michael AC, Cui XT. Dexamethasone retrodialysis attenuates microglial response to implanted probes in vivo. Biomaterials. 2016;87:157–169.

43. Zhong Y, Bellamkonda RV. Dexamethasone-coated neural probes elicit attenuated inflammatory response and neuronal loss compared to uncoated neural probes. Brain Res. 2007; 1148:15–27.

44. Spataro L, Dilgen J, Retterer S, Spence AJ, Isaacson M, Turner JN, Shain W. Dexamethasone treatment reduces astroglia responses to inserted neuroprosthetic devices in rat neocortex. Exp Neurol. 2005;194(2):289–300.

45. Nesbitt KM, Varner EL, Jaquins-Gerstl A, Michael AC. Microdialysis in the rat striatum: effects of 24 h dexamethasone retrodialysis on evoked dopamine release and penetration injury. ACS Chem Neurosci. 2015;6(1):163–173.

46. Jaquins-Gerstl A, Shu Z, Zhang J, Liu Y, Weber SG, Michael AC. Effect of dexamethasone on gliosis, ischemia, and dopamine extraction during microdialysis sampling in brain tissue. Anal Chem. 2011;83(20):7662–7667.

47. Nesbitt KM, Jaquins-Gerstl A, Skoda EM, Wipf P, Michael AC. Pharmacological mitigation of tissue damage during brain microdialysis. Anal Chem. 2013;85(17):8173–8179.

48. Zhou Y, Ling EA, Dheen ST. Dexamethasone suppresses monocyte chemoattractant protein-1 production via mitogen activated protein kinase phosphatase-1 dependent inhibition of Jun n-terminal kinase and p38 mitogen-activated protein kinase in activated rat microglia. J Neurochem. 2007;102(3): 667–678.

49. Wen ZH, Wu GJ, Chang YC, Wang JJ, Wong CS. Dexamethasone modulates the development of morphine tolerance and expression of glutamate transporters in rats. Neuroscience. 2005;133(3):807–817.

50. Hue CD, Cho FS, Cao S, Dale Bass CR, Meaney DF, Morrison B 3rd. Dexamethasone potentiates in vitro blood-brain barrier recovery after primary blast injury by glucocorticoid receptor-mediated upregulation of zo-1 tight junction protein. J Cereb Blood Flow Metab. 2015;35(7):1191–1198.

51. Thal SC, Schaible EV, Neuhaus W, Scheffer D, Brandstetter M, Engelhard K, Wunder C, Forster CY. Inhibition of proteasomal glucocorticoid receptor degradation restores dexamethasone-mediated stabilization of the blood-brain barrier after traumatic brain injury. Crit Care Med. 2013;41(5):1305–1315.

52. Zhang Z, Fauser U, Schluesener HJ. Dexamethasone suppresses infiltration of rhoa+ cells into early lesions of rat traumatic brain injury. Acta Neuropathol. 2008;115(3):335–343.

53. Zhang Z, Zhang Z, Artelt M, Burnet M, Schluesener HJ. Dexamethasone attenuates early expression of three molecules associated with microglia/macrophages activation following rat traumatic brain injury. Acta Neuropathol. 2007;113(6): 675–682.

54. Chen X, Zhang KL, Yang SY, Dong JF, Zhang JN. Glucocorticoids aggravate retrograde memory deficiency associated with traumatic brain injury in rats. J Neurotrauma. 2009; 26(2):253–260.

55. Giulian D, Chen J, Ingeman JE, George JK, Noponen M. The role of mononuclear phagocytes in wound healing after traumatic injury to adult mammalian brain. J Neurosci. 1989;9(12): 4416–4429.

56. Hanna RN, Shaked I, Hubbeling HG, Punt JA, Wu R, Herrley E, Zaugg C, Pei H, Geissmann F, Ley K, et al. Nr4a1 (nur77) deletion polarizes macrophages toward an inflammatory phenotype and increases atherosclerosis. Circ Res. 2012;110(3): 416–427.

57. Guilliams M, Ginhoux F, Jakubzick C, Naik SH, Onai N, Schraml BU, Segura E, Tussiwand R, Yona S. Dendritic cells, monocytes and macrophages: a unified nomenclature based on ontogeny. Nat Rev Immunol. 2014;14(8):571–578.

58. Auffray C, Fogg D, Garfa M, Elain G, Join-Lambert O, Kayal S, Sarnacki S, Cumano A, Lauvau G, Geissmann F. Monitoring of blood vessels and tissues by a population of monocytes with patrolling behavior. Science. 2007;317(5838):666–670.

59. Pei L, Castrillo A, Chen M, Hoffmann A, Tontonoz P. Induction of nr4a orphan nuclear receptor expression in macrophages in response to inflammatory stimuli. J Biol Chem. 2005;280(32):29256–29262.

60. Misharin AV, Cuda CM, Saber R, Turner JD, Gierut AK, Haines GK, 3rd, Berdnikovs S, Filer A, Clark AR, Buckley CD, et al. Nonclassical ly6c(-) monocytes drive the development of inflammatory arthritis in mice. Cell Rep. 2014;9(2):591–604.

61. Xiao G, Sun T, Songming C, Cao Y. Nr4a1 enhances neural survival following oxygen and glucose deprivation: an in vitro study. J Neurol Sci. 2013;330(1–2):78–84.

62. Zhao Y, Bruemmer D. Nr4a orphan nuclear receptors: Transcriptional regulators of gene expression in metabolism and vascular biology. Arterioscler Thromb Vasc Biol. 2010; 30(8):1535–1541.